photooxidized, a conclusion consistent with their role as iron ligands as deduced from both X-ray studies. Since both histidine-77 and -73 occur in the same chymotryptic peptide, we are not able to deduce which if either is susceptible to photooxidation. The third photooxidized histidine may not be one unique histidine but a summation of partially oxidized iron-bound histidines; however, this interpretation is not consistent with the appearance of three unique histidines in the NMR.

Acknowledgments

We thank Dr. A. Bothner-By and the NMR Facility for Biomedical Studies at Carnegie-Mellon for making it possible to obtain the 250-MHz proton correlation spectra and Dr. Ken Seamons for generating the theoretical NMR spectra of apohemerythrin.

References

Boeri, E., & Ghiretti-Magaldi, A. (1957) *Biochim. Biophys. Acta 23*, 489–493.
Dadok, J., & Sprecher, R. F. (1974) *J. Magn. Reson. 13*, 243–248.
Easley, C. W. (1965) *Biochim. Biophys. Acta 107*, 386–388.
Ernst, R. R. (1966) *Adv. Magn. Reson. 2*, 1–135.
Fan, C. C., & York, J. L. (1969) *Biochem. Biophys. Res. Commun. 36*, 365–372.
Fan, C. C., & York, J. L. (1972) *Biochem. Biophys. Res. Commun. 47*, 472–476.
Fermi, E. (1930) *Z. Phys. 60*, 320–333.
Ferrell, R. E., & Kitto, G. B. (1971) *Biochemistry 10*, 2923–2929.
Fortune, W. B., & Mellon, M. G. (1938) *Ind. Eng. Chem., Anal. Ed. 10*, 60–64.
Golding, R. M., Mok, K. F., & Duncan, J. F. (1966) *Inorg. Chem. 5*, 774–778.
Hendrickson, W. A. (1978) *Nav. Res. Rev. 31*, 1–20.
Hendrickson, W. A., Klippenstein, G. L., & Ward, K. B. (1975) *Proc. Natl. Acad. Sci. U.S.A. 72*, 2160–2164.
Hudson, A., & Whitfield, H. J. (1966) *Chem. Commun. 17*, 606–607.
Klippenstein, G. L. (1972) *Biochemistry 11*, 372–379.
Klippenstein, G. L., Cote, J. L., & Ludlam, S. E. (1976) *Biochemistry 15*, 1128–1136.
Klotz, I. M. (1967) *Methods Enzymol. 11*, 576–580.
Klotz, I. M., Klotz, T. A., & Fiess, H. A. (1957) *Arch. Biochem. Biophys. 68*, 284–299.
Li, N. C., Tang, P., & Mathur, R. (1961) *J. Phys. Chem. 65*, 1074–1076.
Loehr, J. S., Lammers, P. J., Brimhall, B., & Hermodson, M. A. (1978) *J. Biol. Chem. 253*, 5726–5731.
Mann, T., & Leone, E. (1953) *Biochem. J. 53*, 140–148.
Markley, J. L. (1973) *Biochemistry 12*, 2245–2250.
Markley, J. L., & Ibanez, I. B. (1978) *Biochemistry 17*, 4627–4640.
Markley, J. L., Finkenstadt, W. R., Dugas, H., Leduc, P., & Drapeau, G. R. (1975) *Biochemistry 14*, 998–1005.
Moss, T. H., Moleski, C., & York, J. L. (1971) *Biochemistry 10*, 840–842.
Okamura, M. Y., Klotz, I. M., Johnson, C. E., Winter, M. R. C., & Williams, R. J. P. (1969) *Biochemistry 8*, 1951–1958.
Ozols, M., & Strittmatter, P. (1966) *J. Biol. Chem. 241*, 4793–4797.
Rill, R. L., & Klotz, I. M. (1970) *Arch. Biochem. Biophys. 136*, 507–514.
Rill, R. L., & Klotz, I. M. (1971) *Arch. Biochem. Biophys. 147*, 226–241.
Roberts, G. C. K., Meadows, D. H., & Jardetzky, O. (1969) *Biochemistry 8*, 2053–2056.
Stenkamp, R. E., Sieker, L. C., Jensen, L. H., & McQueen, J. E. (1978) *Biochemistry 17*, 2499–2504.
Subramanian, A. R., Holleman, J. W., & Klotz, I. M. (1968) *Biochemistry 7*, 3859–3867.
Takashima, Y., & Tateishi, Y. (1965) *Bull. Chem. Soc. Jpn. 38*, 1688–1693.
York, J. L., & Bearden, A. J. (1970) *Biochemistry 9*, 4549–4554.
York, J. L., & Fan, C. C. (1971) *Biochemistry 10*, 1659–1665.
York, J. L., & Roberts, M. P. (1976) *Biochim. Biophys. Acta 420*, 265–278.

Resonance Raman Studies of Pyrocatechase–Inhibitor Complexes†

Lawrence Que, Jr.,* Robert H. Heistand II,‡ Ruth Mayer, and A. Lawrence Roe

ABSTRACT: The resonance Raman spectra of native pyrocatechase and its benzoate and phenolate complexes were investigated by using the available lines of an argon and a krypton laser. The data provide evidence for the presence of two distinct tyrosines coordinated to the active-site iron. The two tyrosines exhibit different ν_{CO} values which show maximum resonance enhancements at different excitation wavelengths. Moreover, one tyrosine is more susceptible to changes in the active-site environment. Pyrocatechase is the only example thus far among iron–tyrosinate proteins where the tyrosines coordinating the iron are distinguishable.

The intradiol dioxygenases, pyrocatechase (EC 1.13.1.1) and protocatechuate 3,4-dioxygenase (EC 1.13.1.3), catalyze the cleavage of catechols to *cis,cis*-muconic acids with the incorporation of the elements of molecular oxygen (Nozaki, 1974). The enzymes have a high-spin ferric center in the active site and exhibit visible spectra with absorbance maxima near 450 nm ($\epsilon \sim 3000$–4000 M^{-1} cm^{-1} Fe^{-1}). Recent resonance Raman studies (Tatsuno et al., 1978; Keyes et al., 1978; Felton et al., 1978; Que & Heistand, 1979; Bull et al., 1979) have assigned this visible absorption band as arising from a tyrosinate-to-iron charge-transfer interaction resulting in the enhancement of several tyrosinate vibrational modes, similar to those found for the transferrins and uteroferrin (Gaber et al.,

† From the Department of Chemistry, Cornell University, Ithaca, New York 14853. *Received January 2, 1980.* This work was supported by National Institutes of Health Grant GM25422.
‡ NIH Predoctoral Trainee (GM07273), 1978–1980.

0006-2960/80/0419-2588$01.00/0

1974, 1979; Tomimatsu et al., 1976; Keyes et al., 1978). All these proteins exhibit similar visible spectra and appear to comprise a new class of iron proteins having tyrosinate coordination (Keyes et al., 1978).

Resonance Raman spectroscopy has also been helpful in understanding the enzyme–substrate and enzyme–substrate–O_2 complexes of the dioxygenases. Anaerobic substrate addition to the dioxygenases results in increased absorbance in the long-wavelength region (600–800 nm) of the visible spectra of these enzymes (Fujisawa et al., 1972a; Kojima et al., 1967); resonance Raman studies on these complexes show that this new feature arises from a catecholate-to-iron interaction, providing evidence for substrate binding to the iron (Felton et al., 1978; Que & Heistand, 1979). The catecholate vibrational modes observed are similar to those found in enterobactin and tris(catecholato)ferrate(III) complexes (Salama et al., 1978) and suggest that the substrate chelates to the iron. Studies on the ternary (ESO_2) complex (Fujisawa et al., 1972b) of protocatechuate 3,4-dioxygenase show that the tyrosine environment is perturbed in the intermediate, and no evidence for oxygen or substrate modes is found (Keyes et al., 1979). This indicates that the intermediate involved is not a simple complex of enzyme, substrate, and O_2 but an as yet unidentified product precursor.

In this paper, we have investigated the resonance Raman spectra of pyrocatechase and its benzoate and phenolate complexes and find evidence for the presence of two tyrosines in the iron coordination of the enzyme.

Materials and Methods

All chemicals were obtained commercially and used without further purification. Deuteration of the *o*-chlorophenol at the C-4 and C-6 positions was effected by base-catalyzed exchange in D_2O under N_2 in a sealed NMR tube heated at 140 °C for 4 h. The NMR spectrum of the resulting solution showed >95% deuteration. $Fe(salhis)_2ClO_4 \cdot H_2O$ was prepared according to the procedure of Federer (1977) for the analogous aziridine (replacing imidazole) complex. The ligand, salhis,[1] was prepared by mixing 1.03 g (9.25 mmol) of histamine with 1.13 g (9.30 mmol) of salicylaldehyde in 50 mL of absolute methanol. Addition of 1.68 g (4.63 mmol) of ferrous perchlorate hexahydrate results in a brown solution which immediately changes to purple upon air oxidation. After 12 h of stirring, the methanol was removed under reduced pressure. The resulting purple tar was dissolved in 30 mL of acetone, followed by addition of 30 mL of distilled water. Slow evaporation of the acetone produces a tarry precipitate which is triturated into a solid: yield of the deep purple powder, 2.15 g (3.57 mmol) or 77%; positive Beilstein test for halogen; IR (KBr pellet) 1100 cm^{-1} (very broad, ClO_4^-); mass spectrum, m/z 215 – salhis. Anal. Calcd for $Fe(salhis)_2ClO_4 \cdot H_2O$: C, 47.90; H, 4.35; N, 13.96. Found: C, 47.91; H, 4.40; N, 13.43.

Pyrocatechase was prepared from *Pseudomonas arvilla* C-1 (ATCC 23974) according to published procedures (Fujiwara et al., 1975). The homogeneous enzyme preparation with a specific activity of 30 was used throughout the experiments (Nakai et al., 1979). The apoenzyme was prepared following the procedure for protocatechuate 3,4-dioxygenase (Fujiwara & Nozaki, 1973). Steady-state inhibition kinetic experiments were performed in 50 mM potassium phosphate buffer, pH 7.5, at 25 °C on a Gilson K-1C oxygraph.

[1] Abbreviations used: CD, circular dichroism; EDDHA, ethylenediaminebis(*o*-hydroxyphenyl acetate); ImH, imidazole; salhis, *N*-[2-(4-imidazolyl)ethyl]salicylaldimine.

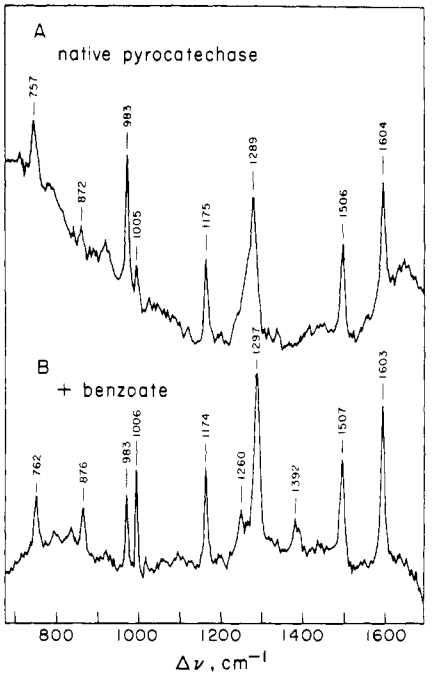

FIGURE 1: Resonance Raman spectra of (A) native pyrocatechase and (B) the pyrocatechase–benzoate complex. Conditions: 647.1-nm excitation, 150–200-mW power, 4-cm^{-1} slit width. Benzoate concentration, 50 mM.

Visible spectra were obtained on a Cary 219 spectrophotometer while CD spectra were obtained on a Cary 60 spectropolarimeter. Resonance Raman spectra were obtained by using a Coherent Radiation Model CR-3 argon ion laser and a Model 500K krypton ion laser. The spectra were recorded on a Spex 1401 spectrometer interfaced with a microprocessor for data handling. Samples were cooled to 4 °C to prevent denaturation of the protein. Treated this way, the enzyme lost a maximum of 10% of its activity after 4 h of irradiation. Prolonged irradiation of the native enzyme at 514.5 nm resulted in a color change and loss of activity. The inhibitor complexes were more stable. Spectra obtained consecutively with the same sample exhibited no significant changes. Spectra were obtained on 40–50 mg/mL protein samples in 50 mM Tris–acetate buffer, pH 8.5, with 0.1 M sulfate as internal standard. Potassium iodide (up to 0.1 M) was added to decrease fluorescence.

Results and Discussion

Pyrocatechase from *Pseudomonas arvilla* C-1 exhibits a visible spectrum with an absorbance maximum near 458 nm. Laser excitation of this chromophore at 647.1 nm yields a resonance Raman spectrum (Figure 1A) with features at 757, 1005, 1175, 1289, 1506, and 1604 cm^{-1} (all polarized). A comparison with the apoenzyme spectrum shows that only the 1005-cm^{-1} peak is not resonance enhanced; this feature is assigned to a phenylalanine ring mode (Lord & Yu, 1970). The latter four peaks have been assigned to tyrosinate vibrations, strikingly similar to features found in the spectra of protocatechuate 3,4-dioxygenase, uteroferrin, and the transferrins. The data for the various proteins are collected in Table I, along with the most likely vibrational assignments. As noted earlier (Gaber et al., 1979), the CO stretch appears to exhibit the most variability, ranging from 1265 cm^{-1} for protocatechuate 3,4-dioxygenase to 1293 cm^{-1} for uteroferrin. Raman studies on phenol indicate that the ionization of phenol to phenolate results in the shift of ν_{CO} from 1249 to 1281 cm^{-1}, suggesting increased double bond character in the C–O bond

Table I: Resonance Raman Frequencies of Phenolate Ring Vibrations in Iron-Tyrosinate Proteins and Model Compounds

	phenolate frequencies (cm^{-1})				ref
ovotransferrin	1605	1504	1270	1170	*a*
serum transferrin	1613	1508	1288	1174	*b*
lactoferrin	1604	1500	1272	1170	*c*
uteroferrin	1607	1504	1293	1173	*d*
protocatechuate 3,4-dioxygenase					
from *Ps. aeruginosa*	1605	1505	1265	1176	*e-g*
from *Ps. putida*	1605	1504	1270	1175	*h*
pyrocatechase	1605	1505	1289	1175	*i, j*
p-cresol-Fe^{3+}, pH 7.0	1618	1488	1222	1180	*e*
p-cresol, pH 14	1607	1490	1276	1176	*e*
$Fe(EDDHA)^-$	1600	1482	1286	1168	*b*
$Fe(salhis)_2ClO_4$, pH 7.0	1625	1476	1337	1159	*j*
	1605	1452	1310	1132	
assignments	ring stretch	ring stretch	CO stretch	CH bend	

[a] Tomimatsu et al. (1976). [b] Gaber et al. (1974). [c] Loehr et al. (1980). [d] Gaber et al. (1979). [e] Tatsuno et al. (1978). [f] Keyes et al. (1978). [g] Felton et al. (1978). [h] Bull et al. (1979). [i] Que & Heistand (1979). [j] This work.

of the phenolate (Tomimatsu et al., 1976). A similar argument may be applied to explain the range of frequencies observed for these proteins. Pyrocatechase would thus fall in the high end of this range. Also noteworthy is the broadness and asymmetry of the 1289-cm^{-1} band in comparison to the other three tyrosine bands; this suggests that the band may consist of more than one feature (vide infra).

The remaining unassigned feature in the resonance Raman spectrum of pyrocatechase is the 757-cm^{-1} peak, which is also observed in the apoenzyme but at lower intensity. This feature is assigned to tryptophan in analogy to protocatechuate 3,4-dioxygenase; the assignment is consistent with fluorescence measurements on the dioxygenases (Nagami & Senoh, 1974; Hou, 1978), indicating the presence of tryptophan in the active sites of these enzymes. Tryptophan, however, is considered a poor iron ligand, and the resonance enhancement observed probably arises from ring-stacking interactions with the iron–tyrosine chromophore (Bull et al., 1979; Loehr et al., 1980).

To probe the active site in more detail, we have investigated the benzoate and phenolate complexes of pyrocatechase. Benzoate is a competitive inhibitor of pyrocatechase (K_i = 6 mM); addition of sufficient benzoate to saturate the active site of the enzyme induces a red shift in the visible spectrum with λ_{max} 505 nm (Figure 2). Resonance Raman spectra of this complex were obtained by using the available lines of an argon and a krypton laser; two of these (647.1 nm, Figure 1B; 514.5 nm, Figure 3, top) are shown. Several features are worth noting. Peaks at 875 and 1260 cm^{-1} appear, while the 1289-cm^{-1} peak is shifted to 1297 cm^{-1}. The 1260- and 1297-cm^{-1} features are symmetric in contrast to the 1289-cm^{-1} band of the native enzyme. Nonresonant vibrational modes of the added benzoate at 1006 and 1392 cm^{-1} are also observed. The excitation profile of the major resonance Raman bands shows a maximum near 600 nm for the peaks at 1605, 1505, and 1175 cm^{-1}, while the 1297-cm^{-1} line peaks near 650 nm and the 1260-cm^{-1} line peaks near 560 nm. These maxima do not coincide with the absorption maximum but instead follow the positive peak in the CD spectrum (Figure 2). This is similar to the excitation profile of enterobactin which maximizes near its CD peak rather than its absorption maximum (Salama et al., 1978). In contrast, transferrin exhibits a complex profile characterized by a vibronic progression at 1000-cm^{-1} intervals (Gaber et al., 1974), and uteroferrin shows

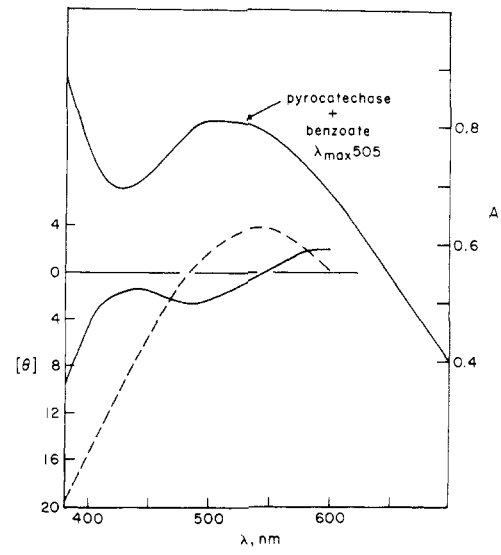

FIGURE 2: (Top) Visible absorption spectrum of the pyrocatechase–benzoate complex. (Bottom) CD spectra of the pyrocatechase–benzoate complex (—) and the pyrocatechase–*o*-chlorophenol complex (- -). Spectra were obtained on 17 mg/mL enzyme in Tris–acetate buffer, pH 8, 25 °C.

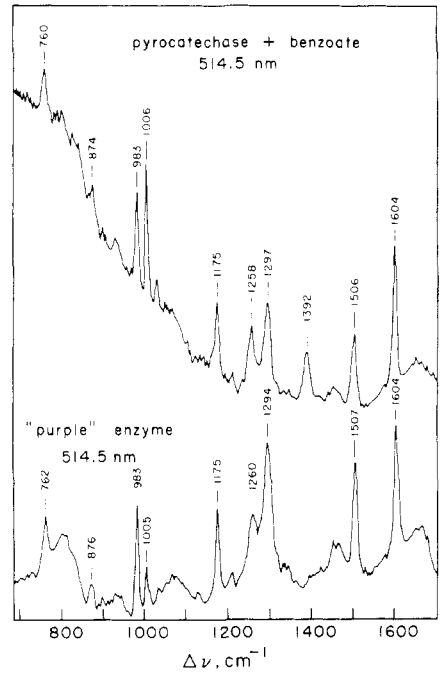

FIGURE 3: Resonance Raman spectra of (top) the pyrocatechase–benzoate complex and (bottom) the "purple" enzyme. Conditions: 514.5-nm excitation, 150–200-mW power, 6-cm^{-1} slit width. Benzoate concentration, 50 mM.

a structureless profile with maximum enhancement coincident with its visible absorption maximum (Gaber et al., 1979).

Phenolates are also competitive inhibitors of pyrocatechase; typical inhibition constants are 500 μM for phenol and 3 μM for *o*-chlorophenol. Addition of phenols to the enzyme effects a blue shift in the visible spectrum; for the *o*-chlorophenol complex, λ_{max} goes from 458 to 440 nm. These are similar to the changes observed in phenolate complexes of protocatechuate 3,4-dioxygenase (Zaborsky et al., 1975; May et al., 1978), and the visible spectra of the two enzymes are compared in Figure 4. The similarity between the two dioxygenases is clear, though they are distinct from each other. One such difference is the slight hump near 600 nm in the spectrum of the pyrocatechase–*o*-chlorophenol complex, sug-

Table II: Resonance Raman Data for Dioxygenase Complexes (700–1700 cm^{-1})

enzyme complex	excitation wavelength (nm)	observed modes (cm^{-1})											ref
pyrocatechase													
native	647.1	1604		1506			1289		1175			757	*a*
+benzoate	647.1	1603		1507			1297	1260	1174	876		762	*a*
	514.5	1604		1506			1297	1258	1175	874		760	*a*
+*o*-chlorophenol	647.1	1605		1507		1301	1289	1260	1175	875		761	*a*
	514.5	1605	1586	1505	1475	1300		1260	1175	874	802	762	*a*
+*o*-chlorophenol-4,6-d_2	647.1	1605		1507		1293	1293	1260	1173	875		763	*a*
	514.5	1605	1573	1506	1472	1291		1259	1174	877	802	762	*a*
+*o*-fluorophenol	647.1	1603		1507		1296	1296	1259	1175	875		760	*a*
+*o*-bromophenol	647.1	1604		1507		1300	1288	1259	1175	874		761	*a*
+2,4,6-trichlorophenol	647.1	1605		1505		1295	1287			872		760	*a*
+phenol	647.1	1603		1505		1289	1289	1260	1175	871		759	*a*
protocatechuate 3,4-dioxygenase													
native	488.0, 514.5	1605		1505				1265	1176	863	834	756	*b-e*
+3-chloro-4-hydroxybenzoate	514.5	1606	1592	1505	1487	1299		1260	1171			759	*d*
+3-fluoro-4-hydroxybenzoate	514.5	1606		1505		1303		1263	1173			760	*d*

[a] This work. [b] Tatsuno et al. (1978). [c] Keyes et al. (1978). [d] Felton et al. (1978). [e] Bull et al. (1979).

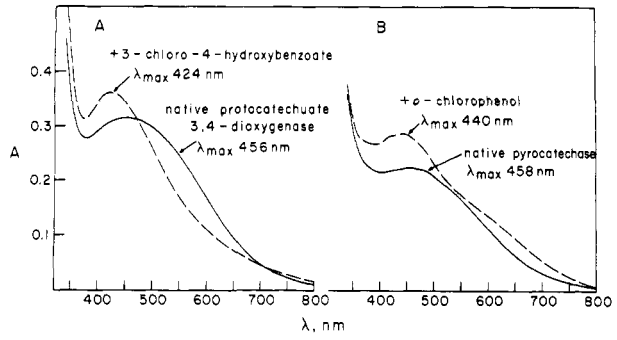

FIGURE 4: Visible absorption spectra of (A) protocatechuate 3,4-dioxygenase and its complex with 3-chloro-4-hydroxybenzoate in Tris-Cl buffer, pH 8, 25 °C, and (B) pyrocatechase and its complex with *o*-chlorophenol in Tris–acetate buffer, pH 8, 25 °C.

gestive of more than one electronic transition.

We have observed the resonance Raman spectra of several phenolate complexes (Table II); those of the *o*-chlorophenol complex are representative (Figure 5). Like the benzoate complex, peaks at 875 and 1260 cm^{-1} emerge. In addition, there are features at 1300, 1475, and 1586 cm^{-1}. These are assigned to the *o*-chlorophenolate; deuteration of the ring protons at the 4 and 6 positions results in the shift of these peaks to lower frequency (Table II). The vibrational assignments for the *o*-chlorophenolate features are probably analogous to those for the tyrosinate peaks in the same frequency range. The excitation profile for this complex is similar in behavior to that of the benzoate complex (Figure 6). The features at 1605, 1505, and 1175 cm^{-1} all show maximum enhancement near the CD maximum (Figure 2) to the red region of the optical maximum while the bands in the ν_{CO} region peak at different wavelengths. The 1289-cm^{-1} band maximizes in the red region and the 1260-cm^{-1} band maximizes in the blue region while the 1301-cm^{-1} feature shows maxima both in the red and blue regions with a minimum near 570 nm. The *o*-chlorophenolate features at 1475 and 1586 cm^{-1} are not evident at 647.1 nm; they begin to emerge at 568.2 nm and maximize near 500 nm like the 1260- and 1301-cm^{-1} peaks. Why the 1475- and 1586-cm^{-1} peaks do not appear at 647.1 nm is not understood.

Lastly, we have observed the spectrum of the native enzyme with 514.5 nm excitation, which exhibits a 1260-cm^{-1} band in addition to the features observed at 647.1 nm. However, the background fluorescence significantly affects the signal-to-noise ratio. Our experiments suggest that this fluorescence

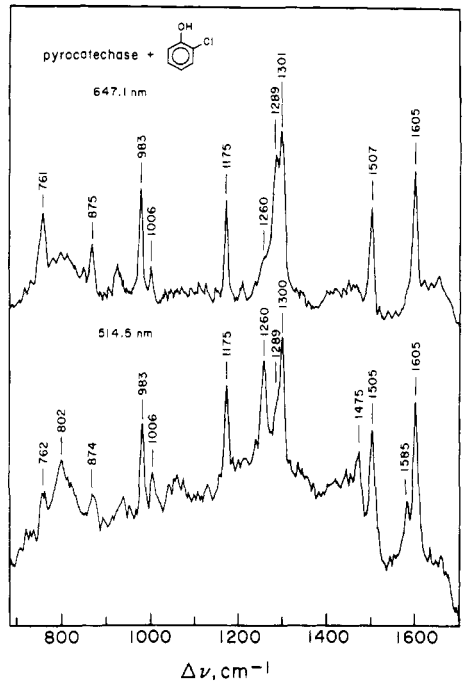

FIGURE 5: Resonance Raman spectra of the pyrocatechase–*o*-chlorophenol complex. Conditions: 647.1-nm excitation, 150–200-mW power, 4-cm^{-1} slit width; 514.5-nm excitation, 150–200-mW power, 6-cm^{-1} slit width. *o*-Chlorophenol concentration, 5 mM.

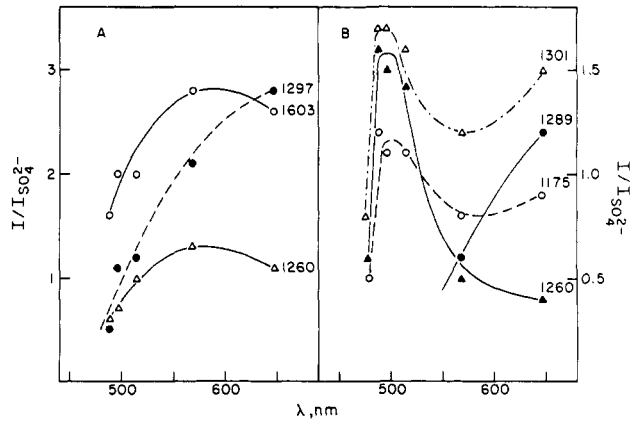

FIGURE 6: Excitation profiles of (A) the pyrocatechase–benzoate complex and (B) the pyrocatechase–*o*-chlorophenol complex. Data points are band peak heights normalized to the 983-cm^{-1} band of SO_4^{2-}. Spectra were not obtainable at 457.9 nm due to fluorescence problems.

is inherent to the enzyme since the addition of inhibitors such as the phenolates and benzoate diminish the fluorescence. Furthermore, prolonged irradiation of the native enzyme at 514.5 nm (80 h) eliminates the fluorescence; this process, however, also changes the originally pink enzyme solution to an inactive purple solution. Similar color changes have been observed with enzyme that has been inactivated by sodium mersalyl or storage at −20 °C for 6 months (Watari et al., 1966). The resonance Raman spectrum of this "purple" enzyme (Figure 3, bottom) exhibits features similar to those of the benzoate complex. What happens during the irradiation is not clear, though the spectral similarity of the "purple" enzyme to the benzoate complex may indicate similar structural changes in the active site; the benzoate-induced changes are reversible, however.

Many of the features of the resonance Raman spectra of pyrocatechase and its complexes can easily be assigned to tyrosinate vibrations by comparison with the spectra of protocatechuate 3,4-dioxygenase, uteroferrin, and the transferrins. There is one important difference—the emergence of a 1260-cm^{-1} feature. In all other proteins studied, only one peak in the ν_{CO} region is observed, unless another phenolate coordinates as in the case of the phenolate complexes of the two dioxygenases (Felton et al., 1978). But in pyrocatechase, we observe peaks at 1260 and ca. 1290 cm^{-1}. That the 1260-cm^{-1} peak is observed without added inhibitor indicates that this mode is inherent to the enzyme. That the 1260-cm^{-1} peak has an excitation profile different from that of the 1290-cm^{-1} peak indicates that there are two different charge-transfer interactions having different λ_{max} values.

Two possible assignments for the 1260-cm^{-1} band immediately come to mind—an imidazole ring breathing mode or another tyrosinate CO stretch. The ubiquity of histidine coordination in the active sites of metalloproteins is well-known (Vallee & Wacker, 1970), making the imidazole assignment resonable. However, the 1260-cm^{-1} band does not arise from imidazole. Resonance Raman studies on copper– and cobalt–imidazole complexes have been reported (Siiman et al., 1974; Tomimatsu et al., 1976; Yoshida et al., 1975; Salama & Spiro, 1978). No enhancement of imidazole modes was observed with visible excitation; only with excitation in the near-ultraviolet (363.8 nm) was some enhancement noted for the cobalt complexes (Salama & Spiro, 1978). This suggests that metal–imidazole charge-transfer interactions occur in the UV region rather than in the visible region. Thus, imidazole would not be expected to contribute to the visible absorption maximum of pyrocatechase. Since no studies of ferric complexes of this type have been reported, we synthesized an iron complex with both phenolate and imidazole functionalities, $Fe(salhis)_2ClO_4 \cdot H_2O$. This complex exhibits a visible spectrum in acetone with λ_{max} 531 nm (ϵ 4100 M^{-1} cm^{-1}). Its resonance Raman bands are assignable to phenolate vibrations (Table I). Salama & Spiro (1978) further point out that N_1 deuteration of the coordinated imidazole in $Co(ImH)_4(ClO_4)_2$ results in a shift of the bands of 1257 and 1336 cm^{-1} to 1244 and 1322 cm^{-1}, respectively. No discernible shifts are observed in D_2O for the iron complex and the pyrocatechase complexes. All the evidence thus argues against an imidazole assignment for the 1260-cm^{-1} peak.

The alternative assignment is that of the ν_{CO} of another coordinated tyrosine, with the corresponding phenyl ring breathing and bending modes coincident with those of the other tyrosine. We noted earlier in our survey of iron–tyrosinate proteins that the ν_{CO} can vary as much as 30 cm^{-1} without affecting the other three vibrations. This assignment would also be consistent with the excitation profiles of the inhibitor complexes. The 1260-cm^{-1} band shows maximum enhancement at higher energy than the 1290-cm^{-1} band. However, the peaks arising from the ring breathing and binding modes, being composites of the two tyrosines, do not follow the profile of either ν_{CO} and, instead, show maximum enhancements at wavelengths between the ν_{CO} maxima.

The 875-cm^{-1} band is tentatively assigned to tyrosine; similar features are found in the spectra of the other metal–tyrosinate proteins. These features may arise from Fermi resonance between a ring breathing vibration and an overtone of an out-of-plane bending mode, resulting in the observation of a doublet, the so-called tyrosine doublet (Siamwiza et al., 1975). In uteroferrin, two peaks (803 and 873 cm^{-1}) are clearly observed (Gaber et al., 1979) while in the various metal-substituted transferrins, only one is well defined, with the other sometimes indiscernible from the noise (Tomimatsu et al., 1976). The Fermi resonance assignment also implies the enhancement of the ν_{16a} fundamental mode of tyrosine at ca. 410 cm^{-1} (Gaber et al., 1979). This has not been observed for uteroferrin or pyrocatechase, so the assignment for the 875-cm^{-1} peak is at best tentative.

In conclusion, our spectral studies suggest the presence of two distinct tyrosines coordinating the active-site iron in pyrocatechase. This distinction is manifested in the observation of two ν_{CO} values in the resonance Raman spectra of the various enzyme complexes. These ν_{CO} values each have their own excitation maximum, indicating the presence of two charge-transfer interactions. The difference between the two tyrosines is also reflected in the sensitivity of one tyrosine to the nature of the inhibitor; the ν_{CO} at 1260 cm^{-1} remains unchanged in all the complexes studied while the other varies from 1289 to 1297 cm^{-1}. Our data on the phenolate complexes indicate that the phenolates bind to the iron without displacing the tyrosines and contribute to both charge-transfer interactions. These complexes exhibit visible absorption maxima near 440 nm, consistent with having three phenolates coordinating the iron (Ackermann & Hesse, 1970). As for the benzoate complex, we have no direct evidence for benzoate binding to the iron since no benzoate modes are resonance enhanced (nor were they expected to be); the spectral changes observed, however, suggest that benzoate coordination is not unlikely. The nature of the other ligands around the iron is currently unknown. Due to its ubiquity in metalloprotein active sites, histidine is the most probable candidate. Examples of nonheme iron proteins with both tyrosine and hisitidine coordination are transferrin (Line et al., 1967; Komatsu & Feeney, 1967) and hemerythrin (Hendrickson et al., 1975; Stenkamp et al., 1976). Interestingly, the Mössbauer parameters of the reduced protocatechuate 3,4-dioxygenase compare well with those of deoxyhemerythrin (Que et al., 1976). Our failure to observe resonance-enhanced imidazole modes is probably not due to the absence of histidine in the iron coordination but more likely due to the higher energies at which the imidazole-to-metal charge-transfer interactions are expected to occur. Perhaps future studies with lasers in the near-ultraviolet will clarify this point.

Acknowledgments

We thank Professor H. A. Scheraga for the use of the Raman spectrometer and J. Widom for experimental assistance.

References

Ackermann, G., & Hesse, D. (1970) *Z. Anorg. Allg. Chem.* *375*, 77–86.

Bull, C., Ballou, D. P., & Salmeen, I. (1979) *Biochem. Biophys. Res. Commun. 87*, 836–841.
Federer, W. (1977) M.S. Thesis, Bucknell University.
Felton, R. H., Cheung, L. D., Phillips, R. S., & May, S. W. (1978) *Biochem. Biophys. Res. Commun. 85*, 844–850.
Fujisawa, H., Uyeda, M., Kojima, G., Nozaki, M., & Hayaishi, O. (1972a) *J. Biol. Chem. 247*, 4414–4421.
Fujisawa, H., Hiromi, K., Uyeda, M., Okuno, S., Nozaki, M., & Hayaishi, O. (1972b) *J. Biol. Chem. 247*, 4422–4428.
Fujiwara, M., & Nozaki, M. (1973) *Biochim. Biophys. Acta 327*, 306–312.
Fujiwara, M., Golovleva, L. A., Saeki, Y., Nozaki, M., & Hayaishi, O. (1975) *J. Biol. Chem. 250*, 4848–4855.
Gaber, B. P., Miskowski, V., & Spiro, T. G. (1974) *J. Am. Chem. Soc. 96*, 6868–6873.
Gaber, B. P., Sheridan, J. P., Bazer, F. W., & Roberts, R. M. (1979) *J. Biol. Chem. 254*, 8340–8342.
Hendrickson, W. A., Klippenstein, G. L., & Ward, K. B. (1975) *Proc. Natl. Acad. Sci. U.S.A. 72*, 2160–2164.
Hou, C. T. (1978) *J. Inorg. Biochem. 8*, 237–243.
Keyes, W. E., Loehr, T. M., & Taylor, M. L. (1978) *Biochem. Biophys. Res. Commun. 83*, 941–945.
Keyes, W. E., Loehr, T. M., Taylor, M. L., & Loehr, J. S. (1979) *Biochem. Biophys. Res. Commun. 89*, 420–427.
Kojima, Y., Fujisawa, H., Nakazawa, A., Nakazawa, T., Kanetsuna, F., Taniuchi, H., Nozaki, M., & Hayaishi, O. (1967) *J. Biol. Chem. 242*, 3270–3278.
Komatsu, S. K., & Feeney, R. E. (1967) *Biochemistry 6*, 1136–1141.
Line, W. F., Grohlich, D., & Bezkarovainy, A. (1967) *Biochemisty 6*, 3393–3402.
Loehr, T. M., Keyes, W. E., & Loehr, J. S. (1980) in *Oxidases and Related Redox Systems* (King, T. E., Mason, H. S., & Morrison, M., Eds.) in press.
Lord, R. C., & Yu, N. T. (1970) *J. Mol. Biol. 50*, 509–524.
May, S. W., Phillips, R. S., & Oldham, C. D. (1978) *Biochemistry 17*, 1853–1860.
Nagami, K., & Senoh, S. (1974) *J. Biochem. (Tokyo) 75*, 389–398.
Nakai, C., Kagamiyama, H., Saeki, Y., & Nozaki, M. (1979) *Arch. Biochem. Biophys. 195*, 12–22.
Nozaki, M. (1974) in *Molecular Mechanisms of Oxygen Activation* (Hayaishi, O., Ed.) pp 135–167, Academic Press, New York.
Que, L., Jr., & Heistand, R. H., II (1979) *J. Am. Chem. Soc. 101*, 2219–2221.
Que, L., Jr., Lipscomb, J. D., Zimmermann, R., Münck, E., Orme-Johnson, N. R., & Orme-Johnson, W. H. (1976) *Biochim. Biophys. Acta 452*, 320–334.
Salama, S., & Spiro, T. G. (1978) *J. Am. Chem. Soc. 100*, 1105–1111.
Salama, S., Stong, J. D., Neilands, J. B., & Spiro, T. G. (1978) *Biochemistry 17*, 3781–3785.
Siamwiza, M. N., Lord, R. C., Chen, M. C., Takamatsu, T., Harada, I., Matsuura, H., & Shimanouchi, T. (1975) *Biochemistry 14*, 4870–4876.
Siiman, O., Young, N. M., & Carey, P. R. (1974) *J. Am. Chem. Soc. 96*, 5583–5585.
Stenkamp, R. E., Sieker, L. C., & Jensen, L. H. (1976) *Proc. Natl. Acad. Sci. U.S.A. 73*, 349–351.
Tatsuno, Y., Saeki, Y., Iwaki, M., Yagi, T., Nozaki, M., Kitagawa, T., & Otsuka, S. (1978) *J. Am. Chem. Soc. 100*, 4614–4615.
Tomimatsu, Y., Kint, S., & Scherer, J. R. (1976) *Biochemistry 15*, 4918–4924.
Valle, B. L., & Wacker, W. E. C. (1970) *Proteins (2nd Ed.) 5*, 1.
Watari, H., Nakazawa, T., Yamano, T., & Hayaishi, O. (1966) in *Biological and Chemical Aspects of Oxygenases* (Bloch, K., & Hayaishi, O., Eds.) pp 369–372, Maruzen, Tokyo.
Yoshida, C. M., Freedman, T. B., & Loehr, T. M. (1975) *J. Am. Chem. Soc. 97*, 1028–1032.
Zaborsky, O. R., Hou, C. T., & Ogletree, J. (1975) *Biochim. Biophys. Acta 386*, 18–25.

Liver Aldolase Anomeric Specificity†

Keith J. Schray,* Elizabeth Ehrhardt Howell, John M. Waud, Stephen J. Benkovic, and Brian A. Cunningham

ABSTRACT: Stopped-flow kinetic studies of liver aldolase and of mixed liver–muscle aldolase catalyzed reactions of fructose 1,6-bisphosphate (FBP) have been carried out and interpreted by computer simulation. These experiments indicate no utilization or binding of the α anomer by the liver enzyme unlike the findings for either the muscle aldolase which binds the α anomer nonproductively or the yeast aldolase which catalyzes its cleavage. Both β-fructose 1,6-bisphosphate and its acyclic keto form may serve as substrates, necessitating the spontaneous anomerization of the α anomer before its utilization. Thus, liver aldolase cleaves 100% of the substrate present in the millisecond time scale because of the inability to bind α-FBP, allowing rapid spontaneous anomerization. This result fulfills earlier predictions of the differing specificities and substrate binding properties for aldolases from yeast, muscle, and liver.

Most enzymes using sugar phosphates have now been examined for their specificity toward the anomeric or acyclic forms of these substrates. Several interesting postulates concerning the role of the observed specificities in metabolic regulation have been put forward (Schray & Benkovic, 1978; Benkovic & Schray, 1976; Wurster & Hess, 1974; Koerner et al., 1977).

Muscle aldolase has been shown by Wurster & Hess (1973) as well as by Schray et al. (1975) to be specific for the β anomer of fructose 1,6-bisphosphate (FBP)[1] and to bind the

† From the Department of Chemistry and the Center for Health Sciences, Lehigh University, Bethlehem, Pennsylvania 18015, and the Department of Chemistry, The Pennsylvania State University, University Park, Pennsylvania 16802. *Received October 11, 1979.* Supported by National Institutes of Health Grants GM-22378 and GM-13306 and Biomedical Support Grant S07 RR 07173.

0006-2960/80/0419-2593$01.00/0